Jin M, Monroig O, Navarro JC, Tocher DR & Zhou Q (2017) Molecular and functional characterisation of two elovl4 elongases involved in the biosynthesis of very long-chain (>C24) polyunsaturated fatty acids in black seabream Acanthopagrus schlegelii, *Comparative Biochemistry and Physiology - B: Comparative Biochemistry*, 212, pp. 41-50.

DOI: 10.1016/j.cbpb.2017.06.008

Title

Molecular and functional characterisation of two *elovl4* elongases involved in the biosynthesis of very long-chain (>C_{24}) polyunsaturated fatty acids in black seabream *Acanthopagrus schlegelii*

Authors

Min Jin[a, b, c], Óscar Monroig[b*], Juan Carlos Navarro[d], Douglas R. Tocher[b], Qi-Cun Zhou[a, c*]

Affiliations

[a] Laboratory of Fish Nutrition, School of Marine Sciences, Ningbo University, Ningbo 315211, China

[b] Institute of Aquaculture, Faculty of Natural Sciences, University of Stirling, Stirling FK9 4LA, Scotland, UK

[c] Mariculture Efficient Healthy Breeding Synergy and Innovation Center of Zhejiang, China

[d] Instituto de Acuicultura Torre de la Sal (IATS-CSIC), 12595 Ribera de Cabanes, Castellón, Spain

***Corresponding authors**

Dr. Óscar Monroig, Tel: +44-1786-467892, oscar.monroig@stir.ac.uk (Ó. Monroig).

Prof. Qi-Cun Zhou, Tel/Fax: +86-574-876-09878, zhouqicun@nbu.edu.cn (Q. -C. Zhou).

Keywords: *Acanthopagrus schlegelii*; biosynthesis; Elongation of very long-chain fatty acid 4 protein, Very long-chain polyunsaturated fatty acids

Accepted for publication in *Comparative Biochemistry and Physiology - Part B: Biochemistry & Molecular Biology* published by Elsevier.

Abstract

Elongation of very long-chain fatty acid (Elovl) 4 proteins are important fatty acyl elongases that participate in the biosynthesis of long-chain (C_{20-24}) and very long-chain ($>C_{24}$) polyunsaturated fatty acids (LC-PUFA and VLC-PUFA, respectively) in teleost fish, especially in marine species. Moreover, knowledge of Elovl4 and other elongases such as Elovl2 has contributed to an advanced understanding of the LC-PUFA biosynthetic pathway in marine fish. In the present study, *elovl4a* and *elovl4b* were cloned from black seabream *Acanthopagrus schlegelii* and functionally characterised using recombinant expression in yeast. The *elovl4a* and *elovl4b* cDNA sequences included open reading frames (ORF) of 969 and 918 base pairs (bp), encoding proteins of 322 and 315 amino acids (aa), respectively. The functional characterisation of *A. schlegelii* Elovl4 proteins showed they were able to utilise all assayed C_{18-22} PUFA substrates except 22:6n-3. Moreover, it was particularly noteworthy that both *A. schlegelii* Elovl4a and Elovl4b proteins had the ability to elongate 20:5n-3 and 22:5n-3 to 24:5n-3, which can be potentially desaturated and β-oxidised to 22:6n-3. Tissue transcript abundance analysis showed the highest expression of *elovl4a* and *elovl4b* in brain and eye, respectively, suggesting these tissues were major sites for VLC-PUFA biosynthesis in black seabream. The functions of the *A. schlegelii* Elovl4-like elongases, Elovl4a and Elovl4b, characterised in the present study, along with those of the Elovl5 and fatty acyl desaturase (Fads2) proteins of *A. schlegelii* characterised previously, provided evidence of the biosynthetic pathways of LC-PUFA and VLC-PUFA in this teleost species.

1. Introduction

Long-chain (C_{20-24}) polyunsaturated fatty acids (LC-PUFA), in particular arachidonic acid (ARA, 20:4n-6), eicosapentaenoic acid (EPA, 20:5n-3) and docosahexaenoic acid (DHA, 22:6n-3), are essential nutrients involved in a variety of important biological processes in vertebrates (Calder, 2006; Castro et al., 2016; McCann and Ames, 2005; NRC, 2011; Simopoulos, 2000). The LC-PUFA profiles of body tissues of animals including fish are primarily reflected by the diet and, to a lesser extend, by endogenous metabolic processes among which LC-PUFA biosynthesis is arguably the most relevant pathway (Tocher, 2003). The LC-PUFA biosynthetic pathways in all vertebrates including fish proceed through enzymatic reactions mediated by fatty acyl desaturases (Fads) and elongation of very long-chain fatty acid (Elovl) enzymes that convert the dietary essential C_{18} PUFA, linoleic acid (LNA, 18:2n-6) and α-linolenic acid (ALA, 18:3n-3), into LC-PUFA such as ARA, EPA and DHA (Monroig et al., 2011a; Castro et al., 2016; Guillou et al., 2010; Jakobsson et al., 2006). Fish species vary in their desaturase and elongase capacity and consequently their ability to efficiently utilise dietary C_{18} PUFA to biosynthesise the physiologically important fatty acids (FA) such as ARA, EPA and DHA. This has become a topic of considerable interest and investigation, particularly for farmed finfish species as aquafeeds are now being formulated with increasing levels of vegetable oils (VO), rich in the C_{18} FA such as LNA and ALA but, unlike the traditionally used fish oil (FO), devoid of LC-PUFA (Turchini et al., 2009). While replacement of FO with non-marine oil sources such as VO has been acknowledged to help increase aquaculture sustainability, this strategy impacts the nutritional value of the farmed products for human consumers (Henriques et al., 2014; Sprague et al., 2016; Shepherd et al., 2017).

63 The Elovl enzymes are the initial and rate-limiting enzymes in the FA elongation complex
64 and are responsible for catalysing the condensation of activated FA with malonyl-CoA required for
65 FA biosynthesis (Nugteren, 1965; Simopoulos, 2000; Leonard et al., 2004; Jakobsson et al., 2006;
66 Guillou et al., 2010). Among the seven members of the Elovl family described in vertebrates
67 (Guillou et al., 2010), only Elovl2, Elovl4 and Elovl5 have been shown to elongate polyunsaturated
68 FA (Monroig et al., 2011a). Elovl5 has been found in a large variety of fish (Castro et al., 2016) and
69 existing evidence suggests that this enzyme is present in virtually all teleost species (Monroig et al.,
70 2016a). In contrast, Elovl2 has a more restricted pattern of distribution and it has been postulated to
71 be absent in Acanthopterygii, a group of teleost fish that encompasses the vast majority of marine
72 fish species currently farmed. Fish Elovl2 enzymes have been functionally characterised from
73 *Danio rerio* (Agaba et al., 2004), *Salmo salar* (Morais et al., 2009), *Oncorhynchus mykiss* (Gregory
74 and James, 2014) and *Clarias gariepinus* (Oboh et al., 2016). These studies confirmed that, unlike
75 Elovl5 enzymes, Elovl2 enzymes elongate C_{22} PUFA and thus convert 22:5n-3 to 24:5n-3, a key
76 reaction for DHA biosynthesis through the so-called "Sprecher shunt" (Sprecher, 2000). Indeed, the
77 lack of *elovl2* gene in marine farmed fish was hypothesised as one of the contributing factors
78 responsible for the low ability of most farmed marine fish to biosynthesise DHA (Morais et al.,
79 2009).

80 The Elovl4 enzymes are the PUFA elongases that have been investigated most recently
81 (Castro et al., 2016). Elovl4 are key enzymes involved in the biosynthesis of very long-chain ($>C_{24}$)
82 PUFA (VLC-PUFA), important components of retina, brain and testis in vertebrates in which they
83 accumulate primarily through endogenous production (Agbaga et al., 2008, 2010; Aveldaño, 1987,
84 1988, 1993; Castro et al., 2016; Furland et al., 2003, 2007a, b; McMahon et al., 2007; Robinson et

al., 1990; Poulos, 1995; Zadravec et al., 2011). Fish Elovl4 enzymes have been characterised in both model species such as zebrafish *D. rerio* (Monroig et al., 2010) and commercially important species (Carmona-Antoñanzas et al., 2011; Monroig et al., 2011b, 2012; Kabeya et al., 2015; Li et al., 2017). Genomic information currently available from a range of teleosts suggests that, unlike other vertebrates, fish possess two distinct types of Elovl4 termed Elovl4a and Elovl4b according to the nomenclature of the *D. rerio* orthologues (Monroig et al., 2010). However, with the exception of the *D. rerio* Elovl4a, all Elovl4 cDNA sequences investigated to date encode Elovl4b-like elongases. It is interesting to note that some fish Elovl4 enzymes showed the ability to elongate 22:5n-3 to 24:5n-3, suggesting that these enzymes have the potential to contribute to DHA biosynthesis and thus partly compensate for the abovementioned absence of Elovl2 in marine species (Monroig et al., 2011b). Therefore, in addition to their major role in VLC-PUFA biosynthesis, some teleost Elovl4 can contribute to the LC-PUFA biosynthesis thus denoting shared roles in both pathways.

Black seabream (*Acanthopagrus schlegelii*) is a popular marine fish species with an increasingly important farming industry in China, Japan, Korea and other countries in South East Asia (Nip et al., 2003; Gonzalez et al., 2008; Ma et al., 2008, 2013; Shao et al., 2008; Zhou et al., 2010a, b; 2011). Previous studies have demonstrated that *A. schlegelii* possesses a Fads2 with Δ6 desaturase activity (Kim et al., 2011), as well as an Elovl5 with the ability to elongate of C_{18} and C_{20} PUFA (Kim et al., 2012). In order to expand our knowledge of the gene complement and functional activities involved in the biosynthesis of LC-PUFA and VLC-PUFA, we herein report the molecular cloning and functional characterisation of *elovl4a* and *elovl4b* cDNAs from *A. schlegelii*, and their transcript tissue distribution. Furthermore, our findings on Elovl4a and Elovl4b are discussed in conjunction with those previously reported on Fads2 and Elovl5 (Kim et al., 2011,

2012) to describe the potential capability of *A. schlegelii* to utilise alternative, sustainable feeds based on vegetable oils rich in C_{18} PUFA but devoid of LC-PUFA.

2. Materials and methods

2.1 Sample collection, RNA extraction and cDNA synthesis

Tissues including brain, eye, gills, heart, intestine, liver, muscle, spleen and stomach were collected from black seabream *Acanthopagrus schlegelii* (three fish were pooled, n = 3) supplied by a commercial hatchery at Xiangshan Bay, Ningbo, China, and fed a commercial feed. Prior to sampling, nine individuals were anaesthetised with a dose of 100 mg L^{-1} of tricaine methanesulfonate (MS-222). Tissue samples were immediately preserved in RNA protective solution (RNAstore, CWBio, China) and kept at 4 ºC overnight before being stored at −80 °C until further analyses. Total RNA was extracted from *A. schlegelii* tissues using TRIzol Reagent (Takara, Japan) according to the manufacturer's instructions. Quantity of isolated RNA was determined spectrophotometrically (Nanodrop 2000, ThermoFisher Scientific, USA), whereas RNA quality was measured by electrophoresis on a 1.2 % agarose gel. For quantitative reverse-transcriptase polymerase chain reaction (qPCR), complementary DNA (cDNA) was prepared from 1,000 ng of DNAase-treated RNA and synthesised using PrimeScript TM RT Reagent Kit with gDNA Eraser (Perfect Real Time, Takara). For gene cloning, cDNA was synthesised from brain RNA using a cDNA Reverse Transcription Reagent Kit (TransScript® One-Step gDNA Removal and cDNA Synthesis SuperMix, China) following the manufacturer's instructions.

2.2 Molecular cloning of elovl4a and elovl4b full-length cDNAs

128 Cloning of cDNA was carried out using PCR-based methodologies and brain cDNA as
129 template. Degenerate primers ASE4a-F and ASE4a-R (*elovl4a*) and ASE4b-F and ASE4b-R
130 (*elovl4b*) (Table 1), designed on conserved regions of teleost *elovl4a* and *elovl4b* orthologues
131 available in the GenBank database, were used for amplification of the first fragment of the cDNA
132 sequences. For *elovl4a*, the sequences from *D. rerio* (gb|NM_200796.1|), *Larimichthys crocea*
133 (gb|XM_010740021.2|) and *Oreochromis niloticus* (gb|XM_003443672.4|) were aligned using the
134 ClustalWtool (Clustal Omega) at the web server (http://www.ebi.ac.uk/Tools/msa/clustalo/) for
135 degenerate primer design. Similarly, sequences from *D. rerio* (gb|NM_199972.1|), *Rachycentron*
136 *canadum* (gb|HM026361.1|), *S. salar* (gb|HM208347.1|), and *Siganus canaliculatus*
137 (gb|JF320823.1|) were aligned for design of degenerate primers for cloning the first fragment of the
138 *A. schlegelii elovl4b*. PCR conditions consisted of an initial denaturation step at 95 °C for 3 min,
139 followed by 35 cycles of denaturation at 95 °C for 30 s, annealing at 58 °C for 30 s, extension at
140 72 °C for 1 min 30 s, followed by a final extension at 72 °C for 5 min. The PCR fragments were
141 purified using the Illustra GFX PCR DNA and Gel Band Purification kit (GE Healthcare, Little
142 Chalfont, UK), and they were sequenced (GATC Biotech Ltd., Konstanz, Germany).

143 In order to obtain the full-length open reading frame (ORF) sequences, two-round (nested)
144 Rapid Amplification of cDNA Ends (RACE) PCR was performed using the SMART RACE cDNA
145 Amplification Kit (Clontech, USA) and using DNase treated RNA from brain. All primers are
146 presented in Table 1. In the first round of PCR, a target gene-specific primer and the Universal
147 Primer A Mix (UPM, provided in the kit) were used according to the manufacturer's instructions
148 (Advantage® 2 PCR Kit, Clontech, USA). In the second round of PCR, another specific primer set
149 and Nested Universal Primer (NUP) (provided in the kit) were used. The PCR parameters were as

follows: 35 cycles of 95 °C for 30 s, 59 °C for 30 s, and 72 °C for 30 s, with an additional initial denaturation at 95 °C for 3 min and a final extension at 72 °C for 5 min. Potential positive fragments were cloned into the pEASY-T3 cloning vector (pEASY-T3 Cloning Kit, Transgen Biotech, Beijing, China) and sequenced as described above. The full-length cDNA sequences were obtained by aligning the first and RACE PCR product sequences using DNAMAN software (Version 6.0, Lynnon BioSoft. Inc., USA).

2.3 Sequence, phylogenetic and 2D topology analysis of the A. schlegelii Elovl4 elongases proteins

The amino acid (aa) sequences encoded by the *A. schlegelii elovl4a* and *elovl4b* cDNAs were deduced using ORFfinder available at NCBI (https://www.ncbi.nlm.nih.gov/orffinder/) and further confirmed using DNAMAN software (Version 6.0, Lynnon BioSoft. Inc., USA). The deduced aa sequences of the newly cloned *A. schlegelii elovl4a* and *elovl4b* and those from a variety of species across vertebrate lineages were used for phylogenetic analysis using the neighbour-joining method with MEGA 6.0 (http://www.megasoftware.net/) (Saitou and Nei, 1987). Confidence in the resulting tree branch topology was measured using bootstrapping through 1,000 replications. The obtained *A. schlegelii* aa sequences were submitted to TOPCONS (http://topcons.net/) for prediction of 2D topology set up with default parameters (Tsirigos et al., 2015), and the Protter web application vision 1.0 (http://wlab.ethz.ch/protter) was used for results visualisation (Omasits et al., 2014).

2.4 Functional characterization of A. schlegelii Elovl4a and Elovl4b cDNAs using heterologous expression in yeast

The functions of the *A. schlegelii* Elovl4a and Elovl4b proteins were determined by expressing the ORF in *Saccharomyces cerevisiae* according to the methodology described by Li et al. (2017).

172 Briefly, PCR fragments corresponding to the ORF of *A. schlegelii elovl4a* and *elovl4b* were
173 amplified from cDNA synthesised from brain RNA, using the high fidelity *Pfu* DNA polymerase
174 (Promega, USA) with primers containing *Bam*HI (forward) and *Xho*I (reverse) restriction sites
175 (Table 1). PCR conditions consisted of an initial denaturation step at 95 °C for 2 min, followed by
176 35 cycles of denaturation at 95 °C for 30 s, annealing at 58 °C for 30 s, extension at 72 °C for 2 min
177 20 s, followed by a final extension at 72 °C for 5 min. The obtained DNA fragments were purified
178 as described above, digested with the appropriate restriction enzymes, and ligated into similarly
179 digested pYES2 yeast expression vector (Invitrogen, Life Technologies™, USA) to produce the
180 constructs pYES2-*elovl4a* or pYES2-*elovl4b*. Sequence accuracy of pYES2-*elovl4a* and
181 pYES2-*elovl4b* constructs was confirmed by DNA sequencing (GATC Biotech Ltd).

182 Yeast competent cells InvSc1 (Invitrogen, Life Technologies™, USA) were transformed with
183 either pYES2-*elovl4a,* pYES2-*elovl4b* or with empty pYES2 (control) using the S.c. EasyComp™
184 Transformation Kit (Invitrogen, Life Technologies™, USA). Selection of yeast containing the
185 pYES2 constructs was performed on *S. cerevisiae* minimal medium minus uracil (SCMM-ura)
186 plates. One single yeast colony transformed with either pYES2-*elovl4a*, pYES2-*elovl4b* or empty
187 pYES (control) was grown in SCMM-ura broth for 2 days at 30 °C, and subsequently subcultured in
188 individual Erlenmeyer flasks at an initial optical density measured at a wavelength of 600 nm
189 (OD600) of 0.4. Subcultures were then grown until an OD600 of 1 was reached, point at which
190 galactose (2%, w/v) and a PUFA substrate supplemented as sodium salts were added
191 (Lopes-Marques et al., 2017). PUFA substrates including C_{18} (18:4n-3 and 18:3n-6), C_{20} (20:5n-3
192 and 20:4n-6), and C_{22} (22:5n-3, 22:6n-3 and 22:4n-6) were used at final concentrations of 0.5 mM
193 (C_{18}), 0.75 mM (C_{20}) and 1.0 mM (C_{22}) to compensate for differential uptake related to fatty acyl

194 chain length (Oboh et al., 2016). After 2 days, the yeast cells were harvested, washed and
195 homogenised in chloroform/methanol (2:1, v/v) containing 0.01% butylated hydroxytoluene (BHT)
196 and stored at −20 °C until further analysis. All PUFA substrates (98 – 99 % pure) used for the
197 functional characterisation assays, except for stearidonic acid (18:4n-3), were obtained from
198 Nu-Chek Prep, Inc. (Elysian, MN, USA). Stearidonic acid (99 % pure) and yeast culture reagents
199 including galactose, nitrogen base, raffinose, tergitol NP-40 and uracil dropout medium were
200 purchased from Sigma-Aldrich (Poole, UK).

201 The analyses of FA compositions of transgenic yeast expressing the *A. schlegelii elovl4a* and
202 *elovl4b* were performed as described by Li et al. (2017). Briefly, total lipid from yeast was extracted
203 by homogenisation in chloroform/methanol (2:1, v/v) containing 0.01% BHT as antioxidant. Fatty
204 acyl methyl esters (FAME) were subsequently prepared, extracted and purified (Monroig et al.,
205 2013) and identified and quantified using GC-MS as described by Li et al. (2017). The elongation
206 of exogenously supplemented PUFA substrates (18:4n-3, 18:3n-6, 20:5n-3, 20:4n-6, 22:5n-3,
207 22:6n-3 and 22:4n-6) was calculated by the step-wise proportion of substrate PUFA converted to
208 elongated product as [areas under the peak of first product and longer chain products/ (areas under
209 the peak of all products with longer chain than substrate + substrate area under the peak)] x 100.

210 *2.5 Transcript abundance analysis*

211 Expression of the *A. schlegelii elovl4* genes was determined by qPCR on RNA samples
212 prepared as described above. Specific primers for the target genes *elovl4a* and *elovl4b* used for
213 qPCR were designed using Primer Premier 5.0 (Table 1). The primer specificity assay of the target
214 genes was performed according to Bustin et al. (2010). Primer specificity was checked by
215 systematically running melting curve assays after the qPCR program and running the qPCR

products on a 1 % (w/v) agarose gel. Amplifications were performed using Luminaris Color Higreen qPCR master mix (Thermo Scientific, CA, USA) following the manufacturer's instructions. The qPCR assays were performed in a total volume of 20 μL, containing 1.0 μL of each primer (final concentration of 10 pmol μL^{-1}), 10 μL of Luminaris Color Higreen qPCR master mix, 5 μL of 1/ 20 diluted cDNA and 3 μL DEPC-water. The thermal-cycling conditions for qPCR were as follows: 50 °C for 2 min, 95 °C for 10 min followed by 40 cycles of 95 °C for 15 s, 60 °C for 30 s and 72 °C for 30 s. No template control (NTC) containing no cDNA were systematically run in all plates. Standard curves were generated using six different dilutions (in triplicate) of the cDNA samples, and the amplification efficiency was analysed using the equation $E=10^{(-1/Slope)}-1$ (Jothikumar et al., 2006). The amplification efficiencies of all genes were approximately equal and ranged from 87 to 105 %. For normalisation purposes, the stability of potential references genes including *β-actin* and *18S rRNA* was tested using Bestkeeper (Pfaffl et al., 2004). The results confirmed that *β-actin* was very stable (stability value was 0.33) and was subsequently used as a reference gene to normalise the expression levels of the candidate genes. The mRNA expression levels of *elovl4a* and *elovl4b* in different tissue of *A. schlegelii* were normalised relative to the expression of *β-actin* calculated by Standard Curve (Pfaffl) methods (Pfaffl, 2001), and liver was set as a control group in this study.

2.6 Statistical analysis

Tissue relative gene expression (qPCR) results were expressed as mean normalised ratios (± SEM) corresponding to the ratio between the copy numbers of the target genes (*elovl4a* and *elovl4b*) and the copy numbers of the reference gene, *β-actin*. All the relative transcript abundance values were analysed after log2 transformation (Lin et al. 2008; Hellemans and Vandesompele, 2011). The

238 homogeneity of variances (Levene's test) was checked prior to one-way analysis of variance
239 (ANOVA) test. Differences in gene expression among tissues were analysed by ANOVA followed
240 by Tukey's HSD test at a significance level of $P \leq 0.05$ (IBM SPSS Statistics 20).

241

242 **3. Results**

243 *3.1 Sequence and phylogenetic analysis of the newly cloned A. schlegelii elovl4 cDNAs*

244 The *A. schlegelii elovl4a* and *elovl4b* ORF sequences had, respectively, 969 base pair (bp) and
245 918 bp encoding proteins of 322 and 315 aa, respectively (Fig. 1). Both the *A. schlegelii* Elovl4a
246 (GeneBank accession: KY348832) and Elovl4b proteins (GeneBank accession: KU372150)
247 contained the conserved histidine box motif (HXXHH), as well as the predicted endoplasmic
248 reticulum (ER) retention signal at their carboxyl end in agreement with other Elovl4 family
249 members (Zhang et al., 2003) (Fig. 1). Hydropathy analysis indicated that both predicted proteins
250 have seven transmembrane domains (Fig. 2). The deduced *A. schlegelii* Elovl4a and Elovl4b aa
251 sequences were submitted to PFam and BLASTp to identify the main protein domains. The PFam
252 searcher identified only one main domain typical of the Elovl4 family (30 - 257 aa) for both
253 predicted proteins (Fig. 2). Moreover, BLASTp searches showed that the deduced *A. schlegelii*
254 Elovl4a aa sequence had the highest identity scores with Elovl4a-like sequences from other fish
255 species including those from *L. crocea* (gb|XP_010738323.2|, 98 % identity), *O. niloticus*
256 (gb|XP_003443720.1|, 95 % identity) and *D. rerio* (gb|NP_957090.1|, 80 % identity). Moreover, the
257 deduced *A. schlegelii* Elovl4b aa sequence had the highest identity scores with Elovl4b-like
258 elongases from *Epinephelus coioides* (gb|AHI17192.1|, 96 % identity), *Nibea mitsukurii*

(gb|AJD80650.1|, 96 % identity), *S. canaliculatus* (gb|ADZ73580.1|, 96 % identity), *R. canadum* (gb|ADG59898.1|, 95 % identity) and pufferfish *Takifugu rubripes* (gb|XP_003971605.1|, 93 % identity). Both *A. schlegelii* Elovl4a and Elovl4b aa sequences were 67 % identical with each other (Fig. 1). In agreement, phylogenetic analysis showed that both *A. schlegelii* Elovl4 sequences formed two distinct clusters that included either Elovl4a or Elovl4b sequences from a range of teleost species (Fig. 3). The non-teleost Elovl4 proteins formed a separate group, with Elovl2 and Elovl5 proteins clustering even more distantly from Elovl4 sequences (Fig. 3).

3.2 Functional characterisation of the A. schlegelii Elovl4a and Elovl4b proteins in yeast

Functional characterisation of the *A. schlegelii* Elovl4a and Elovl4b proteins were carried out in yeast cells expressing their ORF and grown in the presence of potential Elovl substrates, namely C_{18} (18:4n-3 and 18:3n-6), C_{20} (20:5n-3 and 20:4n-6) and C_{22} (22:5n-3, 22:4n-6 and 22:6n-3) PUFA (Table 2). The FA composition of the yeast transformed with empty pYES2 vector (control) was characterised by having 16:0, 16:1n-7, 18:0, 18:1n-9 and 18:1n-7 as major components, together with whichever exogenously added PUFA (data not shown). This is consistent with *S. cerevisiae* possessing no PUFA elongase activity as reported previously (Agaba et al., 2004). In contrast, yeast cells expressing the ORF of the *A. schlegelii elovl4a* and *elovl4b* were able to utilise the assayed PUFA substrates to produce elongation products whose chain lengths reached in some cases C_{36} (Table 2). Among exogenously added substrates, both Elovl4a and Elovl4b had higher conversions towards C_{22} and C_{20} substrates compared to C_{18} substrates (Table 2). One exception to this pattern was DHA (22:6n-3), which was only marginally elongated by Elovl4a although polyenoic elongation products including 32:6n-3 were detected (Table 2). Indeed, the endogenous production of PUFA with chain lengths > C_{24} in yeast supplemented with exogenously supplemented PUFA

281 allowed us to estimate the efficiency of the *A. schlegelii* Elovl4 enzymes towards potential
282 VLC-PUFA substrates that are not commercially available. Thus, our results showed that
283 conversions towards C_{26-32} VLC-PUFA substrates were particularly high for certain substrates and
284 Elovl4 isoforms (Table 2). Interestingly, both *A. schlegelii* Elovl4a and Elovl4b proteins had the
285 ability to elongate 20:5n-3 and 22:5n-3 to 24:5n-3 (Table 2), a key intermediate of DHA
286 biosynthesis via the Sprecher pathway (Sprecher, 2000).

287 *3.3 Tissue distribution of A. schlegelii elovl4a and elovl4b transcripts*

288 Tissue distribution analysis of *A. schlegelii elovl4a* and *elovl4b* transcripts revealed that they
289 have a widespread tissue distribution, with transcripts detected in all tissues analysed (Fig. 4). For *A.*
290 *schlegelii elovl4a*, the highest transcript level was measured in brain ($P < 0.05$), with eye ranked
291 second with higher transcript levels ($P < 0.05$) compared to all other tissues. With regards to *A.*
292 *schlegelii elovl4b*, eye was found to have a significantly higher transcript level compared to any
293 other analysed tissue, followed by brain and gill (Fig. 4). These results suggested that brain and eye
294 were the main tissue sites for Elovl4 function in black seabream *A. schlegelii*.

295

296 **4. Discussion**

297 FO was traditionally one of the major dietary ingredients in feeds for carnivorous marine fish,
298 as it supplies the FA required to satisfy essential FA requirements, specifically the LC-PUFA
299 including EPA, DHA and ARA (Tocher, 2003). However, due to its limited availability and
300 high-cost, FO has been increasingly replaced in fish feeds by VO (Nasopoulou and Zabetakis, 2012;
301 Henriques et al., 2014; Sprague et al., 2016). Hence, it is essential to clarify the LC-PUFA

302 biosynthesis pathway in farmed fish species to fully understand to what extent VO lacking
303 LC-PUFA can be utilised to satisfy essential FA requirements in that particular species. The present
304 study focused on expanding our knowledge of LC-PUFA (C_{20-24}) and VLC-PUFA (> C_{24})
305 biosynthesis in black seabream *A. schlegelii* by characterising two Elovl4 elongases involved in
306 these pathways (Castro et al., 2016).

307 The results of the present study demonstrated that the two Elovl cDNA sequences cloned from
308 *A. schlegelii* encoded Elovl4 proteins since both BLASTp and PFam searchers revealed typical
309 domains of Elovl4 family members (Marchler-Bauer et al., 2017; Oh et al., 1997). Furthermore,
310 each cDNA correspondingly showed high aa sequence identities with either Elovl4a or Elovl4b-like
311 sequences from teleosts, confirming that the herein studied Elovl4 sequences were indeed
312 orthologues of *elovl4a* and *elovl4b*. The presence of two distinct *elovl4*-like sequences have been
313 hypothesised to be a common trait among teleosts (Castro et al., 2016), in contrast to the presence
314 of one single ELOVL4-encoding gene in mammals (Zhang et al., 2003). Consistently, phylogenetic
315 analysis clustered the *A. schlegelii* Elovl4 proteins separately from each other despite the fact that
316 both deduced protein sequences share common features. On one hand, the *A. schlegelii* Elovl4
317 deduced proteins included a histidine box (HXXHH) described in Elovl4 from other fish species
318 (Carmona-Antoñanzas et al., 2011; Kabeya et al., 2015; Li et al., 2017; Monroig et al., 2010, 2011b,
319 2012) and also characteristic of desaturase and hydrolase enzymes containing a di-iron-oxo cluster
320 (Fe-O-Fe) involved in the coordination of electron reception during FA elongation (Jakobsson et al.,
321 2006). On the other hand, the *A. schlegelii* Elovl4 proteins contained a ER retrieval signal at the C
322 terminus, a pattern linked to elongases with a role in LC-PUFA biosynthesis (Cook and McMaster,
323 2004) and typically shared among members of the microsomal Elovl4 family (Zhang et al., 2003).

Furthermore, the results of membrane protein structure predictions revealed that both *A. schlegelii* Elovl4a and Elovl4b aa sequences have seven transmembrane-spanning domains. Although this result was different from previous studies reporting the presence of five (Li et al., 2017) and six transmembrane-spanning domains (Kabeya et al., 2015), it is clear that Elovl4 proteins are mostly hydrophobic consistent with an integral membrane protein with several putative transmembrane domains (Zhang et al., 2003).

The functional analyses confirmed that both *A. schlegelii* Elovl4a and Elovl4b proteins play major roles in the biosynthesis of VLC-PUFA as they were both able to elongate a range of PUFA substrates and produce polyenoic FA whose chain lengths reached in some cases C_{36}. With the exception of the nibe croaker *N. mitsukurii* Elovl4 (Kabeya et al., 2015), all functionally characterised Elovl4 proteins from fish species showed similar elongation capabilities (Carmona-Antoñanzas et al., 2011; Li et al., 2017; Monroig et al., 2010, 2011b, 2012), consistent with the functions described in mammals (Agbaga et al., 2008) and, recently, aquatic invertebrates such as the cephalopod *Octopus vulgaris* (Monroig et al., 2017). An interesting finding was that the *A. schlegelii* Elovl4a and Elovl4b elongases had the ability to elongate 20:5n-3 and 22:5n-3 to 24:5n-3, which is a key intermediate in the biosynthesis of 22:6n-3 via the Sprecher pathway (Sprecher, 2000). Whereas such elongation capability had been described previously in fish Elovl4b-like enzymes (Monroig et al., 2010, 2011b, 2012; Kabeya et al., 2015; Li et al., 2017), functional characterisation of the zebrafish Elovl4a protein suggested that this protein may have lower preference towards PUFA substrates including 22:5n-3 (Monroig et al., 2010). Therefore, it was noteworthy that the present study confirmed, at least in *A. schlegelii*, that Elovl4a protein activity can result in the production of 24:5n-3 and, hence, potentially contribute to 22:6n-3

346 biosynthesis through the Sprecher pathway. While further research is required to clarify whether
347 this is a more common trait among marine fish Elovl4a protein, it is clear that possessing two
348 Elovl4 with the ability to elongate 22:5n-3 to 24:5n-3 offers a substantial adaptive advantage in
349 species that have lost *elovl2* during evolution (Leaver et al., 2008). This is actually the case in
350 *Acanthopterygii*, the teleost group that *A. schlegelii* and virtually all commercially important farmed
351 marine fish species belong to. It is worth noting that, despite their potential role in the DHA
352 biosynthetic pathway, Elovl4 proteins do not appear to elongate DHA efficiently (Monroig et al.,
353 2010). This is partly confirmed in the present study as the *A. schlegelii* Elovl4a protein only
354 marginally (0.5 %) elongated DHA (22:6n-3) to 24:6n-3. In contrast, the *A. schlegelii* Elovl4b
355 protein was able to elongate DHA and produce 32:6n-3, a VLC-PUFA found in retinal
356 phosphatidylcholine (PC) in gilthead seabream (Monroig et al., 2016b). Such an elongation ability
357 of Elovl4b protein, together with the presence of 32:6n-3 in fish retina, was consistent with the
358 tissue distribution results, which indicated the high transcript abundance of *elovl4b* in eye (retina)
359 suggesting this was a major tissue site of VLC-PUFA biosynthesis in *A. schlegelii*.

360 As discussed above, the highest transcript level of *A. schlegelii elovl4b* was detected in eye and,
361 previously, zebrafish embryos showed high transcript level of *elovl4b* in retina and pineal gland
362 (Monroig et al., 2010), tissues that possess photoreceptor cells in fish (Falcón and Henderson, 2001;
363 Catalá, 2010). The specific functions of VLC-PUFA are not fully understood, but their structure
364 combining those of PUFA at one end and saturated FA at the other, allow particular conformational
365 structures within photoreceptor cell membranes (Agbaga et al., 2010). Brain appears as another
366 major site for VLC-PUFA biosynthesis in *A. schlegelii*, with the highest transcript level of *elovl4a*
367 and second highest for *elovl4b*. High transcript abundances of *elovl4*-like sequences were also

368 reported in embryos (Monroig et al., 2010) and later developmental stages (Carmona-Antoñanzas et
369 al., 2011; Li et al., 2017; Monroig et al. 2010; 2011a, 2012). Although the identification of
370 VLC-PUFA in fish is partly anecdotal (Monroig et al., 2016b; Poulos, 1995), the tissue distributions
371 of Elovl4 reported here along with those of other fish species reported previously
372 (Carmona-Antoñanzas et al., 2011; Li et al., 2017; Monroig et al. 2010; 2011b, 2012) are in
373 agreement with studies on mammals confirming that VLC-PUFA play major roles in retina
374 (Aveldaño, 1987, 1988) and brain (Robinson et al., 1990). The present results suggested that current
375 practices in aquafeed formulation, reducing the inclusion of dietary FO and therefore the levels of
376 VLC-PUFA precursors, could have implications on key biological processes such as vision and
377 brain function.

378 Functional data reported herein for the newly characterised Elovl4 proteins, along with those
379 of the Fads2 and Elovl5 published previously (Kim et al., 2010, 2011), enable us to predict the
380 biosynthetic pathways of LC-PUFA and VLC-PUFA in black seabream *A. schlegelii* (Fig. 5).
381 Previous studies reported that *A. schlegelii* possesses a Fads2 with Δ6 desaturase activity, which
382 could produce 18:3n-6 and 18:4n-3 from 18:2n-6 and 18:3n-3, respectively (Kim et al., 2011). In
383 addition, the *A. schlegelii* Elovl5 was confirmed to have the ability to elongate C_{18} (18:3n-6 and
384 18:4n-3) and C_{20} (20:4n-6 and 20:5n-3) PUFA (Kim et al., 2012). Furthermore, in the present study,
385 we functionally characterised the Elovl4a and Elovl4b proteins from *A. schlegelii*, with the results
386 showing that both Elovl4a and Elovl4b proteins have the capacity to elongate some of the $C_{18\text{-}22}$
387 PUFA up to C_{36}. However, the other biosynthetic pathways of LC-PUFA have been characterised in
388 other marine fish but not been confirmed in *A. schlegelii,* such as Elovl5 elongase activity towards
389 C_{18} (18:2n-6 and 18:3n-3), Δ8 desaturase activity of Fads2 towards C20 (20:2n-6 and 20:3n-3), Δ5

desaturase activity of Fads2 towards C_{20} (20:3n-6 and 20:4n-3), and Δ4 desaturase activity towards C_{22} (20:4n-6 and 20:5n-3) (Castro et al., 2016; Li et al., 2010). Overall, therefore, the LC-PUFA and VLC-PUFA biosynthetic pathways of *A. schlegelii* as described in Fig. 5 must be regarded as preliminary and further investigations are required to confirm or otherwise the presence of further activities.

In conclusion, *A. schlegelii* possesses two distinct Elovl4-like elongases termed as Elovl4a and Elovl4b proteins based on their homology to the zebrafish orthologues. Phylogenetic and 2D structural analysis confirmed that the *A. schlegelii* Elovl4a and Elovl4b proteins possessed all the features of Elovl4 protein family members including a histidine box (HXXHH), ER retrieval signal. Functional analysis indicated that both *A. schlegelii* Elovl4a and Elovl4b proteins were involved in the biosynthesis of VLC-PUFA, since they were able to elongate a variety of exogenously added PUFA substrates to produce polyenes whose chain lengths of up to C_{36} in some cases. Furthermore, both *A. schlegelii* Elovl4a and Elovl4b proteins have the functional capability to potentially participate in DHA biosynthesis from EPA through the Sprecher pathway by producing 24:5n-3 for further Δ6 desaturation. However, DHA itself did not appear to be a major substrate for the *A. schlegelii* Elovl4a protein, although the Elovl4b protein able to elongate DHA up to 32:6n-3. Eye and brain were found to be major sites of Elovl4 expression in *A. schlegelii* and thus likely tissue sites of VLC-PUFA biosynthesis, highlighting the importance of these FA on key physiological processes such as vision and brain function, and the potential importance of adequate dietary supply of VLC-PUFA precursors for farmed fish species.

Conflict of Interest

411 The authors declare that no competing interests exist.

412 **Acknowledgments**

413 This research was supported by the National Natural Science Foundation of China (Grant Nos.
414 31272670 and 41476125), Major Spark Plan Project of the National Ministry of Science and
415 Technology (2014GA701001), the Open Fund of Zhejiang Provincial Top Key Discipline of
416 Aquaculture in Ningbo University, K.C. Wong Magna Fund and K.C. Wong Education Foundation
417 at Ningbo University. This research was further supported by the Ministerio de Economía y
418 Competitividad (LONGFAQUA project, AGL2013-40986-R) and the Generalitat Valenciana
419 (PROMETEOII/2014/085 project).

420

421 **References**

422 Agaba, M., Tocher, D.R., Dickson, C., Dick, J.R., Teale, A.J., 2004. Zebrafish cDNA encoding
423 multifunctional fatty acid elongase involved in production of eicosapentaenoic (20:5n-3) and
424 docosahexaenoic (22:6n-3) acids. Mar. Biotechnol. 6, 251-261.

425 Agbaga, M., Brush, R.S., Mandal, M.N.A., Henry, K., Elliott, M.H. Anderson, R.E., 2008. Role of
426 Stargardt-3 macular dystrophy protein (ELOVL4) in the biosynthesis of very long chain fatty
427 acids. Proc. Natl. Acad. Sci. 105, 12843-12848.

428 Agbaga, M-P., Mandal, M.N.A.; Anderson, R.E., 2010. Retinal very long-chain PUFAs: new
429 insights from studies on ELOVL4 protein. J. Lipid Res. 51, 1624-42.

430 Aveldaño, M.I., 1987. A novel group of very long chain polyenoic fatty acids in dipolyunsaturated
431 phosphatidylcholines from vertebrate retina. J. Biol. Chem. 262, 1172-1179.

432 Aveldaño, M.I., 1988. Phospholipid species containing long and very long polyenoic fatty acids
433 remain with rhodopsin after hexane extraction of photoreceptor membranes. Biochemistry 27,
434 1229-1239.

435 Aveldaño, M.I., Robinson, B.S., Johnson, D., Poulos, A., 1993. Long and very long chain
436 polyunsaturated fatty acids of the n-6 series in rat seminiferous tubules. Active desaturation of
437 24:4n-6 to 24:5n-6 and concomitant formation of odd and even chain tetraenoic and pentaenoic
438 fatty acids up to C_{32}. J. Biol. Chem. 268, 11663-9.

439 Bustin, S. A., Beaulieu, J. F., Huggett, J., Jaggi, R., Kibenge, F. S., Olsvik, P. A., Olsvik, P.A.,
440 Penning, L.C., Toegel, S., 2010. MIQE precis: Practical implementation of minimum standard

441 guidelines for fluorescence-based quantitative real-time PCR experiments. BMC Mol. Biol. 11,
442 74.

443 Calder, P. C. 2006. n-3 polyunsaturated fatty acids, inflammation, and inflammatory diseases. The
444 Am. J. Clin. Nutr. 83, 1505S-1519S.

445 Catalá, A., 2010. The function of very long chain polyunsaturated fatty acids in the pineal gland.
446 Biochim. Biophys. Acta. 1801, 95-99.

447 Carmona-Antoñanzas, G., Monroig, Ó., Dick, J.R., Davie, A., Tocher, D.R., 2011. Biosynthesis of
448 very long-chain fatty acids (C>24) in Atlantic salmon: Cloning, functional characterisation, and
449 tissue distribution of an Elovl4 elongase. Comp. Biochem. Physiol. B 159, 122-129.

450 Castro, L.F.C., Tocher, D.R., Monroig, O., 2016. Long-chain polyunsaturated fatty acid
451 biosynthesis in chordates: Insights into the evolution of Fads and Elovl gene repertoire. Prog.
452 Lipid Res. 62, 25-40.

453 Cook, H.W., McMaster, R.C.R., 2004. Fatty acid desaturation and chain elongation in eukaryotes.
454 In: Vance, D.E., Vance, J.E. Biochemistry of Lipids, Lipoproteins and Membranes. Elsevier,
455 Amsterdam, the Netherlands.

456 Falcón, J., Henderson, R. J., 2001. Incorporation, distribution, and metabolism of polyunsaturated
457 fatty acids in the pineal gland of rainbow trout (*Oncorhynchus mykiss*) in vitro. J. Pineal Res. 31,
458 127-137.

459 Furland, N.E., Maldonado, E.N., Aveldaño, M.I., 2003. Very long chain PUFA in murine testicular
460 triglycerides and cholesterol esters. Lipids 38, 73-80.

461 Furland, N.E., Maldonado, E.N., Aresti, P.A., Aveldaño, M.I., 2007a. Changes in lipids containing
462 long- and very long-chain polyunsaturated fatty acids in cryptorchid rat testes. Biol. Reprod. 77,
463 181-188.

464 Furland, N.E., Oresti, G.M., Antollini, S.S., Venturino, A., Maldonado, E.N., Aveldaño, M.I.,
465 2007b. Very long-chain polyunsaturated fatty acids are the major acyl groups of sphingomyelins
466 and ceramides in the head of mammalian spermatozoa. J. Biol. Chem. 282, 18151-18161.

467 Gonzalez, E.B., Umino, T., Nagasawa, K., 2008. Stock enhancement programme for black
468 seabream, *Acanthopagrus schlegelii* (Bleeker), in Hiroshima Bay, Japan: a review. Aquac. Res.
469 39, 1307-1315.

470 Gregory, M.K., James, M.J., 2014. Rainbow trout (*Oncorhynchus mykiss*) Elovl5 and Elovl2 differ
471 in selectivity for elongation of omega-3 docosapentaenoic acid. Biochim. Biophys. Acta 1841,
472 1656-1660.

473 Guillou, H., Zadravec, D., Martin, P.G.P., Jacobsson, A., 2010. The key roles of elongases and
474 desaturases in mammalian fatty acid metabolism: insights from transgenic mice. Prog. Lipid
475 Res. 49,186-99.

476 Hastings, N., Agaba, M., Tocher, D.R., Leaver, M.J., Dick, J.R., Sargent, J.R., Teale, A.J., 2001. A
477 vertebrate fatty acid desaturase with Δ5 and Δ6 activities. Proc. Natl. Acad. Sci. U. S. A. 98,
478 14304-14309.

479 Hellemans, J., Vandesompele, J., 2011. Quantitative PCR data analysis-unlocking the secret to
480 successful results. In: PCR Troubleshooting and Optimization: The Essential Guide, Caister
481 Academic Press Norwich, UK, pp. 139-150.

Henriques, J., Dick, J.R., Tocher, D.R., Bell, J.G., 2014. Nutritional quality of salmon products available from major retailers in the UK: content and composition of n-3 long-chain polyunsaturated fatty acids. Br. J. Nutr. 112, 964-975.

Jakobsson, A., Westerberg, R., Jacobsson, A., 2006. Fatty acid elongases in mammals: their regulation and roles in metabolism. Prog. Lipid Res. 45, 237-249.

Jackson, M.R., Nilsson, T., Peterson, P.A., 1990. Identification of a consensus motif for retention of transmembrane proteins in the endoplasmic reticulum. EMBO J. 9, 3153-3162.

Jiao, B., Huang, X., Chan, C.B., Zhang, L., D., Cheng, C.H., 2006. The co-existence of two growth hormone receptors in teleost fish and their differential signal transduction, tissue distribution and hormonal regulation of expression in seabream. J. Mol. Endocrinol. 36, 23-40.

Jothikumar, N., Cromeans, T.L., Robertson, B.H., Meng, X.J., Hill, V.R., 2006. A broadly reactive one-step real-time RT-PCR assay for rapid and sensitive detection of hepatitis E virus. J. Virol. Methods 131, 65-71.

Kabeya, N., Yamamoto, Y., Cummins, S. F., Elizur, A., Yazawa, R., Takeuchi, Y., Hagaa, Y., Satoh, S., Yoshizaki, G., 2015. Polyunsaturated fatty acid metabolism in a marine teleost, Nibe croaker *Nibea mitsukurii*: Functional characterization of Fads2 desaturase and Elovl5 and Elovl4 elongases. Comp. Biochem. Physiol. B 188, 37-45.

Kim, S.H., Kim, J.B., Kim, S.Y., Roh, K.H., Kim, H.U., Li, K.R., Jang, Y.S., Kwon, M., 2011. Functional characterization of a delta 6-desaturase gene from the black seabream (*Acanthopagrus schlegeli*). Biotechnol. Lett. 33, 1185-1193.

Kim, S.H., Kim, J.B., Jang, Y.S., Kim, S.Y., Roh, K.H., Kim, H.U., Lee, K.R., Park, J.S., 2012. Isolation and functional characterization of polyunsaturated fatty acid elongase (AsELOVL5) gene from black seabream (*Acanthopagrus schlegelii*). Biotechnol. Lett. 34, 261-268.

Leonard, A.E., Pereira, S.L., Sprecher, H., Huang, Y.S., 2004. Elongation of long-chain fatty acids. Prog. Lipid Res. 43, 36-54.

Leaver, M.J., Bautista, J.M., Björnsson, T., Jönsson, E., Krey, G., Tocher, D.R., Torstensen, B.E., 2008. Towards fish lipid nutrigenomics: current state and prospects for fin-fish aquaculture. Rev. Fish Sci. 16,71-92.

Lin, S.M., Du, P., Huber, W., Kibbe, W.A., 2008. Model-based variance-stabilizing transformation for Illumina microarray data. Nucleic Acids Res. 36(2), e11-e11.

Li, S., Monroig, Ó., Navarro, J. C., Yuan, Y., Xu, W., Mai, K., Tocher, D.R., Ai, Q., 2017. Molecular cloning and functional characterization of a putative Elovl4 gene and its expression in response to dietary fatty acid profiles in orange-spotted grouper *Epinephelus coioides*. Aquac. Res. 48, 538-552.

Li, Y., Monroig, Ó., Zhang, L., Wang, S., Zheng, X., Dick, J.R., You, C., Tocher, D.R., 2010. A vertebrate fatty acyl desaturase with Δ4 activity. Proc. Natl. Acad. Sci. U. S. A. 107, 16840-16845

Lopes-Marques, M., Ozório, R., Amaral, R., Tocher, D. R., Monroig, O., Castro, L.F.C., 2017. Molecular and functional characterization of a *fads2* orthologue in the Amazonian teleost, *Arapaima gigas*. Comp. Biochem. Physiol. B 203, 84-91.

522 Ma, J., Shao, Q., Xu, Z., Zhou, F., 2013. Effect of dietary n-3 highly unsaturated fatty acids on
523 growth, body composition and fatty acid profiles of juvenile black seabream, *Acanthopagrus*
524 *schlegeli* (Bleeker). J. World Aquacult. Soc. 44, 311-325.

525 Ma, J.J., Xu, Z.R., Shao, Q.J., Xu, J.Z., Hung, S.S., Hu, W.L., Zhuo, L.Y., 2008. Effect of dietary
526 supplemental l‐carnitine on growth performance, body composition and antioxidant status in
527 juvenile black seabream, *Sparus macrocephalus*. Aquacult. Nutr. 14, 464-471.

528 Marchler-Bauer, A., Bo, Y., Han, L., He, J., Lanczycki, C. J., Lu, S., Chitsaz, F., Derbyshire, M.K.,
529 Geer, R.C., Gonzales, N.R., Gwadz, M., Hurwitz, D.I., Lu, F., Marchler, G.H., Song, J.S.,
530 Thanki, N., Wang, Z., Yamashita, R.A., Zhang, D., Zheng, C., Geer, L.Y., Gwadz, M., 2017.
531 CDD/SPARCLE: functional classification of proteins via subfamily domain architectures.
532 Nucleic Acids Res. 4, D200-D203.

533 McCann, J. C., Ames, B. N., 2005. Is docosahexaenoic acid, an n- 3 long-chain polyunsaturated
534 fatty acid, required for development of normal brain function? An overview of evidence from
535 cognitive and behavioral tests in humans and animals. Am. J. Clin. Nutr. 8, 281-295.

536 Monroig, Ó., Hontoria, F., Varó, I., Tocher, D.R., Navarro, J.C. 2016b. Biosynthesis of very
537 long-chain (>C24) polyunsaturated fatty acids in juveniles of Gilthead seabream (*Sparus*
538 *aurata*). The 17th International Symposium on Fish Nutrition & Feeding, June 5-10, Sun Valley,
539 Idaho, USA.

540 Monroig, Ó., Llanos, R., Varó, R., Hontoria, F., Tocher D.R., Puig, S., Navarro, J.C., 2017.
541 Biosynthesis of Polyunsaturated Fatty Acids in *Octopus vulgaris*: Molecular cloning and

542 functional characterisation of a stearoyl-CoA desaturase and an elongation of very long-chain
543 fatty acid 4 protein. Mar. Drugs 15, 82.

544 Monroig, Ó., Lopes-Marques, M., Navarro, J.C., Hontoria, F., Ruivo, R., Santos, M.M., Venkatesh,
545 B., Tocher, D.R., Castro, L.F.C., 2016a. Evolutionary functional elaboration of the *Elovl2/5*
546 gene family in chordates. Sci. Rep. 6, 20510.

547 Monroig, Ó., Navarro, J.C., Tocher, D.R., 2011a. Long-chain polyunsaturated fatty acids in fish:
548 recent advances on desaturases and elongases involved in their biosynthesis. In: Cruz-Suarez,
549 L.E., Ricque-Marie, D., Tapia-Salazar, M., Nieto-Lopez, M.G., Villarreal-Cavazos, D.A.,
550 Gamboa-Delgado, J., Hernandez-Hernandez, L.H. (Eds.), Proceedings of the XI International
551 Symposium on Aquaculture Nutrition. Universidad Autónoma de Nuevo León, Monterrey,
552 Nuevo Leon, Mexico, pp. 257-282.

553 Monroig, Ó., Rotllant, J., Cerdá-Reverter, J.M., Dick, J.R., Figueras, A., Tocher, D.R., 2010.
554 Expression and role of Elovl4 elongases in biosynthesis of very long-chain fatty acids during
555 zebrafish *Danio rerio* early embryonic development. Biochim. Biophys. Acta. 1801, 1145-1154.

556 Monroig, Ó., Tocher, D.R., Hontoria, F., Navarro, J.C., 2013. Functional characterisation of a
557 Fads2 fatty acyl desaturase with Δ6/Δ8 activity and an Elovl5 with C16, C18 and C20 elongase
558 activity in the anadromous teleost meagre (*Argyrosomus regius*). Aquaculture 412-413, 14-22.

559 Monroig, Ó., Wang, S., Zhang, L., You, C., Tocher, D.R., Li, Y., 2012. Elongation of long-chain
560 fatty acids in rabbitfish *Siganus canaliculatus*: Cloning, functional characterisation and tissue
561 distribution of Elovl5-and Elovl4-like elongases. Aquaculture 350, 63-70.

562 Monroig, Ó, Webb, K., Ibarra-Castro, L., Holt, G.J., Tocher, D.R., 2011b. Biosynthesis of
563 long-chain polyunsaturated fatty acids in marine fish: Characterization of an Elovl4-like
564 elongase from cobia *Rachycentron canadum* and activation of the pathway during early life
565 stages. Aquaculture 312, 145-153.

566 Morais, S., Monroig, Ó., Zheng, X., Leaver, M., Tocher, D.R., 2009. Highly unsaturated fatty acid
567 synthesis in Atlantic salmon: characterization of ELOVL5- and ELOVL2-like elongases. Mar.
568 Biotechnol. 11, 627-639.

569 National Research Council (NRC), 2011. Nutrient Requirements of Fish and Shrimp. National
570 Academies Press, Washington, DC, pp. 102-125.

571 Nip, T.H., Ho, W.Y., Wong, C.K., 2003. Feeding ecology of larval and juvenile black seabream
572 (*Acanthopagrus schlegeli*) and Japanese seaperch (*Lateolabrax japonicus*) in Tolo Harbour,
573 Hong Kong. Environ. Biol. Fish. 66, 197-209.

574 Nasopoulou, C., Zabetakis, I., 2012. Benefits of fish oil replacement by plant originated oils in
575 compounded fish feeds. A review. LWT-Food. Sci. Technol. 47, 217-224.

576 Nugteren, D.H., 1965. The enzymic chain elongation of fatty acids by rat-liver microsomes.
577 Biochim. Biophys. Acta. 106, 280-290.

578 Oboh, A., Betancor, M.B., Tocher, D.R., Monroig, O., 2016. Biosynthesis of long-chain
579 polyunsaturated fatty acids in the African catfish *Clarias gariepinus*: Molecular cloning and
580 functional characterisation of fatty acyl desaturase (*fads2*) and elongase (*elovl2*) cDNAs.
581 Aquaculture, 462, 70-79.

582 Oh, C. S., Toke, D. A., Mandala, S., & Martin, C. E., 1997. ELO2 and ELO3, Homologues of the
583 *Saccharomyces cerevisiae* ELO1 gene, function in fatty acid elongation and are required for
584 sphingolipid formation. J. Biol. Chem. 272, 17376-17384.

585 Omasits, U., Ahrens, C.H., Müller, S., Wollscheid, B., 2014. Protter: interactive protein feature
586 visualization and integration with experimental proteomic data. Bioinformatics 30, 884-886.

587 Pfaffl, M.W., 2001. A new mathematical model for relative quantification in real-time RT–PCR.
588 Nucleic Acids Res. 29, e45-e45.

589 Pfaffl, M.W., Tichopad, A., Prgomet, C., Neuvians, T.P., 2004. Determination of stable
590 housekeeping genes, differentially regulated target genes and sample integrity:
591 BestKeeper-Excel-based tool using pair-wise correlations. Biotechnol. Lett. 26, 509-515.

592 Poulos, A., 1995. Very long chain fatty acids in higher animals- a review. Lipids 30,1-14.

593 Robinson, B.S., Johnson, D.W., Poulos, A., 1990. Unique molecular species of phosphatidylcholine
594 containing very-long-chain (C24-C38) polyenoic fatty acids in rat brain. Biochem. J. 265,
595 763-767.

596 Saitou, N., Nei, M., 1987. The neighbor-joining method: a new method for reconstructing
597 phylogenetic trees. Mol. Biol. Evol. 4, 406-425.

598 Sargent, J.R., Origin and functions of eggs lipids: nutritional implications. In: Bromage, N.R.,
599 Roberts,R.J., Eds., Broodstock Management and Egg and Larval Quality. Blackwell, London,
600 1995. pp. 353-372.

601 Seelig, A., Seelig, J., 1974. Dynamic structure of fatty acyl chains in a phospholipid bilayer
602 measured by deuterium magnetic resonance. Biochemistry 13, 4839-4845.

603 Shao, Q.J., Ma, J.J., Xu, Z., Hu, W.L., Xu, J.Z., Xie, S.Q., 2008. Dietary phosphorus requirement of
604 juvenile black seabream, *Sparus macrocephalus.* Aquaculture 277, 92-100.

605 Shepherd, C.J., Monroig, O., Tocher, D.R., 2017. Future availability of raw materials for salmon
606 feeds and supply chain implications: the case of Scottish farmed salmon. Aquaculture 467,
607 49-62.

608 Simopoulos, A.P., 2000. Human requirement for N-3 polyunsaturated fatty acids. Poultry Sci. 79,
609 961-970.

610 Song, Y.F., Luo, Z., Pan, Y.X., Zhang, L.H., Chen, Q.L., Zheng, J.L., 2015. Three unsaturated fatty
611 acid biosynthesis-related genes in yellow catfish *Pelteobagrus fulvidraco*: Molecular
612 characterization, tissue expression and transcriptional regulation by leptin. Gene 563, 1-9.

613 Sprague, M., Dick, J.R., Tocher, D.R., 2016. Impact of sustainable feeds on omega-3 long-chain
614 fatty acid levels in farmed Atlantic salmon, 2006-2015. Sci. Rep. 6, 21892

615 Sprecher H., 2000. Metabolism of highly unsaturated n-3 and n-6 fatty acids. Biochim. Biophys.
616 Acta. 1486，219-31.

617 Tocher, D.R., 2003. Metabolism and functions of lipids and fatty acids in teleost fish. Rev. Fish Sci.
618 11, 107-184.

619 Topic Popovic, N., Strunjak-Perovic, I., Coz-Rakovac, R., Barisic, J., Jadan, M., Persin Berakovic,
620 A., Sauerborn Klobucar, R., 2012. Tricaine methane-sulfonate (MS-222) application in fish
621 anaesthesia. J. Appl. Ichthyol. 28, 553-564.

622 Tsirigos, K.D., Peters, C., Shu, N., Käll, L., Elofsson, A., 2015. The TOPCONS web server for
623 consensus prediction of membrane protein topology and signal peptides. Nucleic Acids Res. 43,
624 W401-W407.

625 Turchini, G.M., Torstensen, B.E., Ng, W.K., 2009. Fish oil replacement in finfish nutrition. Rev.
626 Aquacult. 1, 10-57.

627 Wassall, S.R., Stillwell, W., 2008. Docosahexaenoic acid domains: the ultimate non-raft membrane
628 domain. Chem. Phys. Lipids. 153, 57-63.

629 Zhang, X.M., Yang, Z., Karan, G., Hashimoto, T., Baehr, W., Yang, X.J., Zhang, K., 2003. Elovl4
630 mRNA distribution in the developing mouse retina and phylogenetic conservation of Elovl4
631 genes. Mol. Vis. 9, 301-307.

632 Zadravec, D., Tvrdik, P., Guillou, H., Haslam, R., Kobayashi, T., Napier, J.A., Capecchi, M.R.,
633 Jacobsson, A., 2011. Elovl2 controls the level of n-6 28:5 and 30:5 fatty acids in testis, a
634 prerequisite for male fertility and sperm maturation in mice. J. Lipid Res. 52, 245-255.

635 Zheng, X., Ding, Z., Xu, Y., Monroig, O., Morais, S., Tocher, D.R., 2009. Physiological roles of
636 fatty acyl desaturase and elongase in marine fish: characterisation of cDNAs of fatty acyl Δ6
637 desaturase and Elovl5 elongase of cobia (*Rachycentron canadum*). Aquaculture 290, 122-131.

638 Zhou, F., Xiao J.X., Hua Y, Ngandzali B.O., Shao, Q.J., 2011. Dietary l-methionine requirement of
639 juvenile black seabream (*Sparus macrocephalus*) at a constant dietary cystine level. Aquacult.
640 Nutr. 17, 469-481.

641 Zhou, F., Shao, J., Xu, R., Ma, J., Xu, Z., 2010a. Quantitative l‐lysine requirement of juvenile
642 black seabream (*Sparus macrocephalus*). Aquacult. Nutr. 16, 194-204.

643 Zhou, F., Xiong, W., Xiao, J.X., Shao, Q.J., Bergo, O.N., Hua, Y., Cai, X.J., 2010b. Optimum
644 arginine requirement of juvenile black seabream, *Sparus macrocephalus*. Aquac. Res. 41,
645 e418-e430.

646 Zuo, R., Mai, K., Xu, W., Dong, X., Ai, Q., 2016. Molecular cloning, tissue distribution and
647 nutritional regulation of a fatty acyl *elovl5*-like elongase in large yellow croaker, *Larimichthys*
648 *crocea*. Aquac. Res. 47, 2393-2406.

649

650 **Tables**

651

652 Table 1. Sequences of primers used for cDNA cloning, open reading frame (ORF) cloning and
653 tissue expression analysis by qPCR analysis of black seabream *Acanthopagrus schlegelii elovl4a*
654 and *elovl4b*. Restriction sites *Bam*HI and *Xho*I in primers used for cloning into the yeast expression
655 vector pYES2 are underlined.

Aim	Primer name	Primer sequence (5'-3')
Partial fragment	ASE4a-F	TTGCAGACAAGCGGGTGGA
cDNA cloning	ASE4a-R	CCGAAGAGGATGATGAAGGTGA
	ASE4b-F	CAGACAAGSGKGTGGAGA
	ASE4b-R	CCASAGGRTRAACATGG
3'RACE PCR	ASE4a-3R-F1	CCAATGAAGTCAGGGTAGCAGGAGC
	ASE4a-3R-F2	ACTCCCTCATCTGCTACGCCATCAC
	ASE4b-3R-F1	CGTGGAGTTCCTGGATACAGTCTT
	ASE4b-3R-F2	AGGAAGAAGTTCAACCAGGTCAGC
	UPM	CTAATACGACTCACTATAGGGCAAGCAGTGGTATCA ACGCAGAG
5'RACE PCR	ASE4a-5R-R1	GCTCCTGCTACCCTGACTTCATTGG
	ASE4a-5R-R2	CAGCCAGAGGAACAGCAGGTAGGAG
	ASE4b-5R-R1	TTGAGGACCACCATGCTGAAGTTG
	ASE4b-5R-R2	GCCACTTCTCCACCCCCTTGTCTG
	UPM	CTAATACGACTCACTATAGGGCAAGCAGTGGTATCA ACGCAGAGT
ORF cloning	ASE4a-5U-F	ATCCACCACCTCACAGACAT
	ASE4a-3U-R	CTAATCTCTTTTAGCCCTTCCT
	ASE4a-V-F	CCCGGATCCACCATGGAGATTGTCACACATTTG
	ASE4a-V-R	CCGCTCGAGCTAATCTCTTTTAGCCCTTCCTTTC
	ASE4b-5U-F	ACTGAGAGAGGAGTTGGGCA
	ASE4b-3U-R	GCTACTTTTCCACCTTTCCAA
	ASE4b-V-F	CCCGGATCCACCATGGAGGTTGTAACACATTTTG
	ASE4b-V-R	CCGCTCGAGTTACTCCCTTTTCGCTCTTCCC
qPCR	ASE4a-q-F	CTACTCAGACGACCCCAA
	ASE4a-q-R	CACCAGAGCGTGAACATG
	ASE4b-q-F	ATCCAGTTCCACGTGACCAT
	ASE4b-q-R	TCCCATTTTCCTCCACCTCC
	ASβ-actin-F	ACCCAGATCATGTTCGAGACC
	ASβ-actin-R	ATGAGGTAGTCTGTGAGGTCG

656 UPM, Universal Primer A Mix.

657

Table 2. Functional characterisation of *Acanthopagrus schlegelii* Elovl4a and Elovl4b elongases in yeast *Saccharomyces cerevisiae*. Individual conversions towards exogenously supplemented fatty acid (FA) substrates were calculated according to the formula [individual product area under the peak / (all products areas under the peak + substrate area under the peak)] x 100.

		Elovl4a	Elovl4b	
FA substrate	Product	% Conversion	% Conversion	Activity
18:4n-3	20:4n-3	2.5	3.6	C18→36
	22:4n-3	13.3	24.8	C20→36
	24:4n-3	38.2	65.0	C22→36
	26:4n-3	100	91.6	C24→36
	28:4n-3	100	95.5	C26→36
	30:4n-3	29.8	98.0	C28→36
	32:4n-3	76.7	70.6	C30→36
	34:4n-3	N.D.	4.7	C32→36
	36:4n-3	N.D.	N.D.	C34→36
18:3n-6	20:3n-6	4.6	6.5	C18→36
	22:3n-6	37.2	36.6	C20→36
	24:3n-6	40.0	64.6	C22→36
	26:3n-6	56.1	90.0	C24→36
	28:3n-6	100	93.5	C26→36
	30:3n-6	78.6	89.4	C28→36
	32:3n-6	59.0	24.3	C30→36
	34:3n-6	N.D.	3.3	C32→36
	36:3n-6	N.D.	N.D.	C34→36
20:5n-3	22:5n-3	11.6	26.4	C20→36
	24:5n-3	28.5	63.4	C22→36
	26:5n-3	28.7	82.1	C24→36
	28:5n-3	36.5	95.9	C26→36
	30:5n-3	N.D.	99.1	C28→36
	32:5n-3	N.D.	88.3	C30→36
	34:5n-3	N.D.	26.3	C32→36
	36:5n-3	N.D.	1.1	C34→36
20:4n-6	22:4n-6	14.8	27.1	C20→36
	24:4n-6	43.8	59.1	C22→36
	26:4n-6	45.1	73.3	C24→36
	28:4n-6	51.4	89.4	C26→36
	30:4n-6	95.2	94.3	C28→36
	32:4n-6	88.7	50.8	C30→36
	34:4n-6	77.7	5.9	C32→36

	36:4n-6	19.5	N.D.	C34→36
22:5n-3	24:5n-3	6.9	20.3	C22→36
	26:5n-3	23.6	65.5	C24→36
	28:5n-3	35.6	100	C26→36
	30:5n-3	91.4	93.1	C28→36
	32:5n-3	81.2	80.7	C30→36
	34:5n-3	69.0	12.8	C32→36
	36:5n-3	22.2	N.D.	C34→36
22:4n-6	24:4n-6	13.9	28.9	C22→36
	26:4n-6	48.4	69.2	C24→36
	28:4n-6	100	87.9	C26→36
	30:4n-6	59.6	93.9	C28→36
	32:4n-6	85.3	45.4	C30→36
	34:4n-6	75.8	3.4	C32→36
	36:4n-6	22.7	N.D.	C34→36
22:6n-3	24:6n-3	0.5	1.6	C22→36
	26:6n-3	N.D.	100	C24→36
	28:6n-3	N.D.	100	C26→36
	30:6n-3	N.D.	100	C28→36
	32:6n-3	N.D.	48.3	C30→36
	34:4n-3	N.D.	N.D.	C32→36
	36:4n-6	N.D.	N.D.	C34→36

663 N.D., not detected.

664

Figures

Fig. 1. ClustalW alignment of the deduced amino acid sequences of the black seabream *Acanthopagrus schlegelii* Elovl4a and Elovl4b proteins. Identical residues are shaded in black and similar residues are shaded grey. Indicated are the conserved HXXHH histidine box motif and the endoplasmic reticulum (ER) retrieval signal predicted by Zhang et al. (2003).

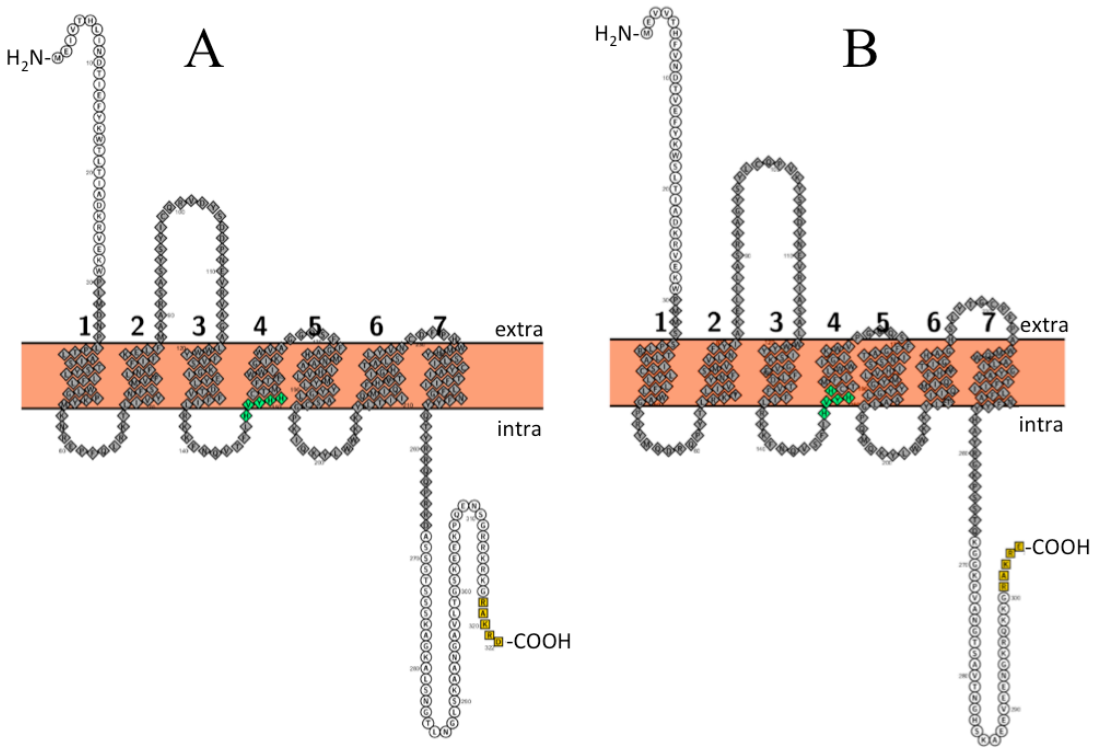

673

674 Fig. 2 Predicted 2D structures of the black seabream *Acanthopagrus schlegelii* Elovl4a (A)
675 and Elovl4b (B) proteins. ◆: Elovl4 protein family domain; ●: His-Box, histidine box motif
676 (HXXHH); ■: Endoplasmic reticulum (ER) retention signal; 1-7: Seven putative
677 transmembrane domains.

678

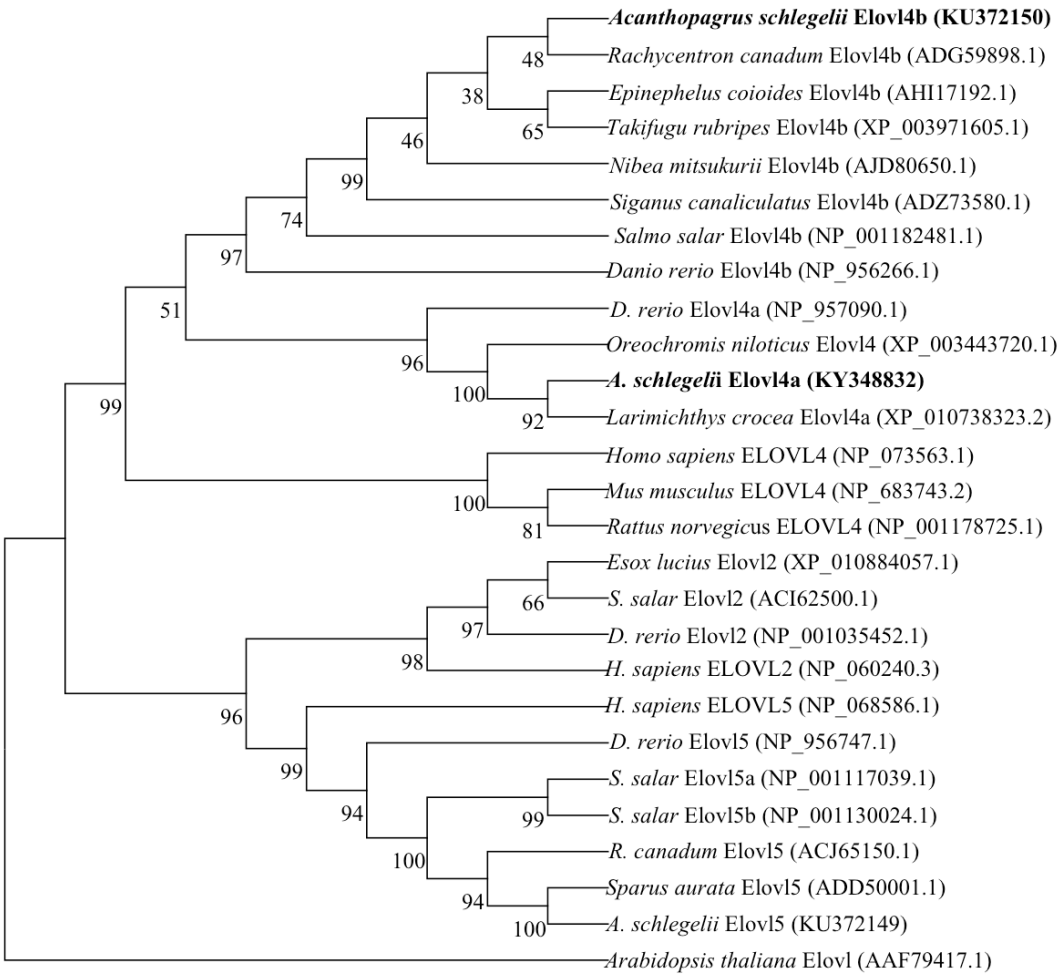

Fig. 3. Phylogenetic tree comparing the black seabream *Acanthopagrus schlegelii* Elovl4a and Elovl4b proteins (bolded) with elongase proteins from other vertebrates. The tree was constructed using the Neighbour-Joining method (Saitou and Nei 1987) using MEGA6. The horizontal branch length is proportional to amino acid substitution rate per site. The numbers represent the frequencies (%) with which the tree topology presented was replicated after 1,000 iterations. The *Arabidopsis thaliana* Elovl sequence was used as outgroup sequence.

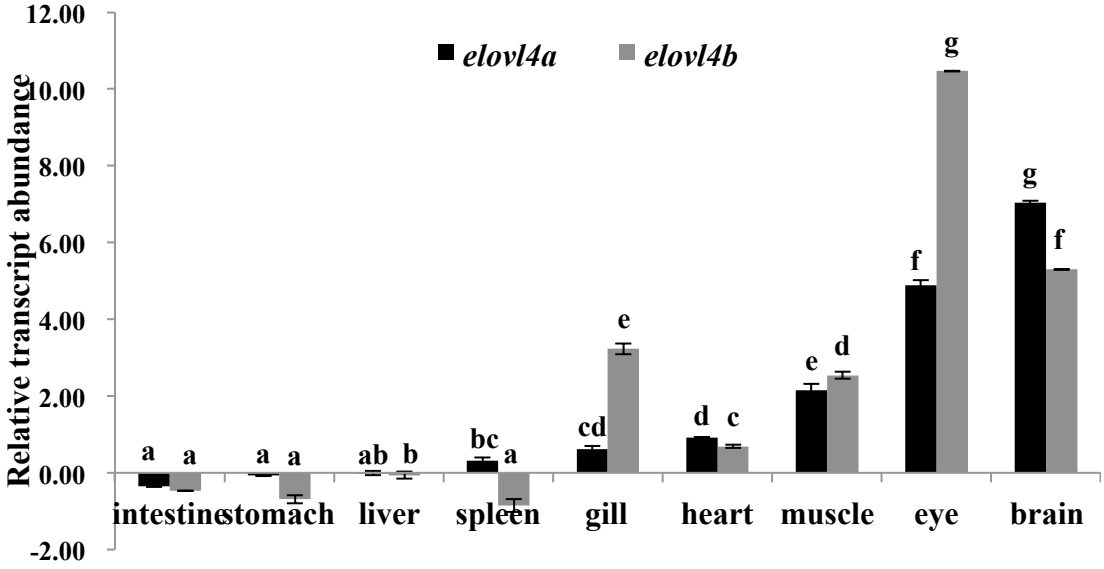

687

688 Fig. 4. Tissue distribution of *elovl4a* and *elovl4b* transcripts in black seabream *Acanthopagrus*
689 *schlegelii.* Bars represent average relative expression values after log2 transformation (Lin et
690 al., 2008; Hellemans and Vandesompele, 2011), with their standard errors (n = 3). The mRNA
691 levels of elovl4a and elovl4b in different tissue of *A. schlegelii* were normalised relative to the
692 expression of *β-actin*, and liver sample was set as a control group. Within each target gene,
693 different letters indicate statistically significant differences in expression levels between
694 tissues ($P \leq 0.05$).

695

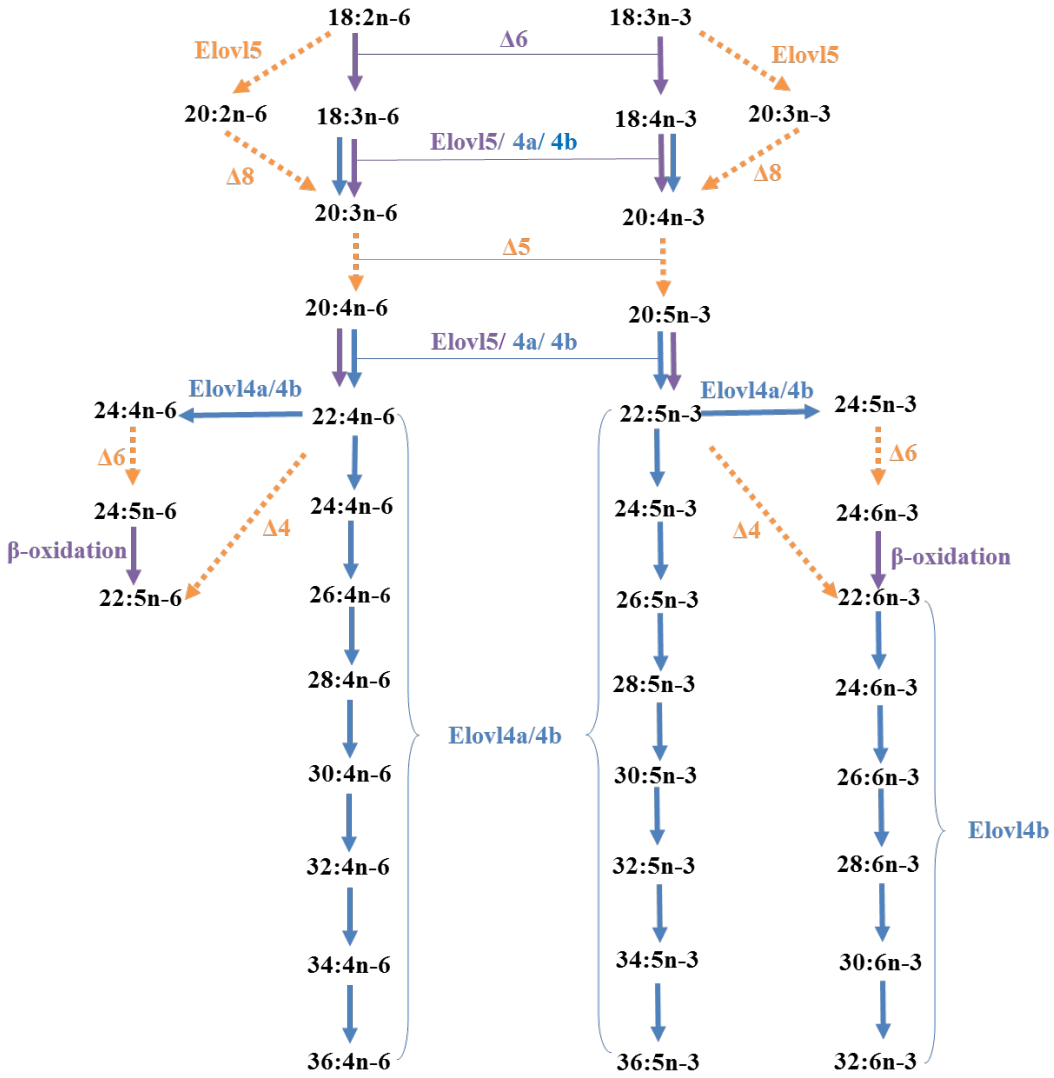

Fig. 5. The long-chain polyunsaturated fatty acid and very long-chain polyunsaturated fatty acid biosynthetic pathway from C_{18} to C_{36} in teleost fish lacking Elovl2. Yellow dashed arrows (➡) represent the pathway confirmed in other marine species (Li et al., 2010; Monroig et al., 2011a; Castro et al., 2016) but not confirmed in *Acanthopagrus schlegelii*. Purple arrows (➡) represent the confirmed pathway in *A. schlegelii* (Kim et al., 2011, 2012) (the β-oxidation process exists naturally), blue arrows(➡) represent the pathways confirmed in the present study.